Journal of Pain Research

Dovepress
Taylor & Francis Group

Open Access Full Text Article

ORIGINAL RESEARCH

Mechanistic Study on the Therapeutic Effects of Juanbi Lijieqing Formula in a Rat Model of Gouty Arthritis with Hyperuricemia

Yifan Lu[1–3,*], Chengyin Lu[1–3,*], Gonghui Jian[2], Hui Xiong[1–3], Yang Shu[1,2]

[1]Orthopedics Department, The First Affiliated Hospital of Hunan University of Chinese Medicine, Changsha, Hunan, 410000, People's Republic of China; [2]Graduate School, Hunan University of Chinese Medicine, Changsha, Hunan, 410208, People's Republic of China; [3]Orthopedics Department, The Second Affiliated Hospital of Hunan University of Chinese Medicine, Changsha, Hunan, 410005, People's Republic of China

*These authors contributed equally to this work

Correspondence: Yang Shu; Hui Xiong, Email 2741926901@qq.com; 3673148112@qq.com

Background: This study evaluated the therapeutic effects and underlying mechanisms of Juanbi Lijieqing Formula (JBLJQF) in a rat model of gouty arthritis with hyperuricemia.

Methods: Forty-two rats were randomly assigned to seven groups: control, model, etoricoxib, benzbromarone, and low-, medium-, and high-dose JBLJQF. General condition, joint swelling, behavioral performance, biochemical markers, and histopathology were assessed. Urate Anion Transporter 1(URAT1) expression was examined via immunofluorescence and Western blot.

Results: JBLJQF improved general condition, reduced joint swelling, and alleviated kidney damage. Medium- and high-dose groups showed enhanced pain threshold and locomotor activity. Serum uric acid, TNF-α, and IL-1β levels were significantly decreased. URAT1 expression was downregulated, suggesting reduced renal urate reabsorption.

Conclusion: JBLJQF exerts anti-inflammatory, uric acid-lowering, and organ-protective effects in gouty arthritis with hyperuricemia, highlighting its potential for clinical application.

Keywords: Juanbi Lijieqing formula, gouty arthritis, hyperuricemia, anti-inflammatory effects, uric acid-lowering

Introduction

Gouty arthritis (GA) is a common metabolic disorder primarily caused by the deposition of monosodium urate crystals in joints and surrounding tissues, often accompanied by acute inflammation and severe pain.[1] Hyperuricemia is a major risk factor for gout and has been shown to not only impair joint health but also contribute to damage in other tissues, such as the kidneys and liver, increasing the risk of comorbidities like cardiovascular diseases and renal dysfunction.[2,3] Therefore, effectively controlling hyperuricemia and alleviating the symptoms of gouty arthritis are of significant clinical importance.

While modern medical treatments for GA, such as nonsteroidal anti-inflammatory drugs (NSAIDs, eg, etoricoxib) and colchicine, have shown efficacy, their long-term use may lead to adverse effects and limited efficacy in controlling uric acid levels.[4,5] Traditional Chinese medicine (TCM) offers a holistic approach that emphasizes addressing both the root cause and symptoms, demonstrating unique advantages in improving symptoms and enhancing patients' quality of life.[6–10]

Juanbi Lijieqing Formula (JBLJQF), a traditional Chinese herbal compound, has shown promising therapeutic effects in the treatment of GA, characterized by its multi-target action and low side-effect profile. Previous studies have indicated that JBLJQF, either alone or in combination with ozone therapy, anti-inflammatory powders, and acupuncture, exerts significant clinical benefits in GA management.[11–14] However, its specific mechanisms of action remain unclear, particularly in modulating inflammatory cytokines, uric acid metabolism, and associated organ damage.

This study aims to systematically evaluate the anti-inflammatory, uric acid-lowering, and organ-protective effects of JBLJQF, providing scientific evidence and novel insights for the clinical treatment of gouty arthritis and hyperuricemia.

Received: 15 January 2025
Accepted: 3 June 2025
Published: 9 June 2025

Materials and Methods

Experimental Animals

A total of 42 male SPF-grade rats, aged 6–8 weeks and weighing 200–220 g, were provided by the Animal Experiment Center of Hunan University of Chinese Medicine (License No. SCXK (Xiang) 2021–0002). The animal experiments in this study were conducted in accordance with the Guide for the Care and Use of Laboratory Animals (8th edition, NIH), and were approved by the Animal Ethics Committee of Hunan University of Chinese Medicine (Approval No. HNUCM 212404–202). The rats were housed in individual cages at the Experimental Animal Center of Hunan University of Chinese Medicine under controlled conditions: temperature of 20–25°C, humidity of 50–70%, and a 12-hour light/dark cycle. Food and water were available ad libitum, and bedding was replaced regularly.

Establishment of a Gouty Arthritis Rat Model

All groups except the control group were fed a high-yeast diet (10%), administered potassium oxonate solution (280 mg/kg·d) and creatinine solution (400 mg/kg·d) via gavage for 14 days. On day 14, rats were anesthetized using inhaled isoflurane (induction concentration of 3–4%). Once the tail pinch and corneal reflexes disappeared, the rats were placed in a prone position for gentle immobilization. Using a 1 mL insulin syringe, 0.2 mL of 20 g/L monosodium urate (MSU) solution was injected into the left knee joint cavity at a 45°–60° angle along the lateral edge of the patellar ligament. The injection endpoint was confirmed by swelling of the contralateral joint capsule. Rats in the control group underwent the same gavage and joint cavity injection procedure but with an equivalent volume of normal saline.

Composition and Preparation of Juanbi Lijieqing Formula

The formula consists of the following ingredients: Atractylodes rhizome (15 g), Phellodendron bark (10 g), Cyathula root (5 g), Cortex fraxini (15 g), Polygonum cuspidatum (15 g), Smilax glabra rhizome (30 g), Spatholobus suberectus stem (30 g), Geranium herb (30 g), Clematis root (15 g), and Dioscorea tokoro rhizome (15 g). All herbal ingredients were purchased from the pharmacy of the First Affiliated Hospital of Hunan University of Chinese Medicine. The herbs were weighed according to the prescription and mixed (See Table 1).

The preparation process involved soaking the mixed herbs in 10 times their volume of distilled water for 30 minutes, followed by reflux extraction for 2 hours using a condensation reflux device. The extract was filtered through gauze, and the residue was subjected to a second extraction with 8 times the volume of distilled water for 1 hour. The two extracts were combined, filtered, and concentrated to the desired concentration using a rotary evaporator.

Animal Grouping and Interventions

Forty-two rats were randomly divided into seven groups (n=6 per group): Control group, Model group, Low-, Medium-, and High-dose Juanbi Lijie Qing Formula (JBLJQ) groups, Positive drug 1 (etoricoxib) group, and Positive drug 2 (benzbromarone) group. Except for the control group, all groups were modeled as described in section 1.2. Interventions

Table 1 Composition of Juanbi Lijieqing Formula

Chinese Name	Latin Name	Medicinal Part	Dosage
Cang Zhu	*Atractylodes Lancea* (Thunb.) DC.	Dried rhizomes	15g
Huang Bo	*Phellodendron chinense* Schneid.	Dried bark	10g
Chuan Niu Xi	*Cyathula officinalis* K.C.Kuan	Dried root	5g
Qin Pi	*Fraxinus chinensis subsp. rhynchophylla* (Hance) A.E.Murray	Dried branch bark or stem bark	15g
Hu Zhang	*Reynoutria japonica* Houtt.	Dried root and rhizome	15g
Tu Fu Ling	*Smilax Glabra* Roxb.	Dried rhizomes	30g
Ji Xue Teng	*Spatholobus suberectus* Dunn	Dried lianoid stem	30g
Lao Guan Cao	*Erodium stephanianum* Willd.	Dried aerial parts	30g
Wei Ling Xian	*Clematis chinensis* Osbeck	Dried root and rhizome	15g
Bi Xie	*Dioscorea collettii var. hypoglauca* (Palib.) S.J.Pei & C.T.Ting	Dried rhizome	15g

started on day 1 post-modeling, with the corresponding drugs administered by gavage once daily for 5 consecutive days. Dosages were calculated using human-to-rat surface area conversion coefficients.(A) Control group: Normal SD rats (n=6), untreated, gavaged with normal saline at 10 mL/kg·d, once daily for 5 days.(B) Model group: Modified GA model rats (n=6), gavaged with normal saline at 10 mL/kg·d, once daily for 5 days.(C) Low-dose JBLJQ group: Modified GA model rats (n=6), gavaged with JBLJQ at 9.25 g/kg·d, once daily for 5 days.(D) Medium-dose JBLJQ group: Modified GA model rats (n=6), gavaged with JBLJQ at 18.5 g/kg·d, once daily for 5 days.(E) High-dose JBLJQ group: Modified GA model rats (n=6), gavaged with JBLJQ at 37 g/kg·d, once daily for 5 days.(F) Positive drug 1 group: Modified GA model rats (n=6), gavaged with etoricoxib at 11 mg/kg·d, once daily for 5 days.(G) Positive drug 2 group: Modified GA model rats (n=6), gavaged with benzbromarone at 5 mg/kg·d, once daily for 5 days. The dosing regimen of JBLJQF (9.25, 18.5, and 37 g/kg·d) was based on the clinically recommended dosage, corresponding to 1, 2, and 4 times the human equivalent dose, respectively. The dosage for the positive control group was determined with reference to previously published studies demonstrating efficacy in similar animal models, and was further adjusted according to the specific requirements of this study.

Reagents

Rabbit anti-URAT1 antibody (Wuhan Sanying, Catalog No. 82964-1-RR); Rabbit anti-ACTIN antibody (Servicebio, Catalog No. GB15003); HRP-goat anti-rabbit secondary antibody (Servicebio, Catalog No. GB23303); Hematoxylin-Eosin (HE) staining kit (Servicebio, Catalog No. G1003); Neutral balsam, xylene, and anhydrous ethanol (China National Pharmaceutical Group Corporation, Catalog Nos. 10004160, 10,023,418, 100,092,683); TNF-α, IL-1β enzyme-linked immunosorbent assay (ELISA) kits (Jianglai Biological, Catalog Nos. JL13202, JL2088).

Sample Collection

(1) Blood: Peripheral blood samples were collected from the jugular vein of rats before modeling and on the first day after modeling. Blood samples were left at room temperature for 30 minutes and then centrifuged at 3000 rpm for 15 minutes at 4°C to separate the serum, which was stored at −80°C until analysis. On the final sampling day, rats were anesthetized with 3% isoflurane, and after the disappearance of the corneal reflex, blood was collected from the abdominal aorta while the rats were fixed in a supine position.

(2) Liver: The abdominal cavity was opened along the midline, and the liver was quickly excised and divided into portions. These were fixed in 4% paraformaldehyde for histological analysis or stored at −80°C for further analysis.

(3) Kidney: The abdominal cavity was opened along the midline, and the kidneys were quickly excised. The left kidney was fixed in 4% paraformaldehyde for histological analysis, while the right kidney was stored at −80°C for future analysis.

(4) Synovium: The left knee of the rat was dissected layer by layer to expose the joint capsule. After opening the joint capsule, a layer of smooth, light yellow soft tissue extending upward from the inferior patella surface was identified as the synovium. This tissue was excised, placed in a −80°C freezer for storage, and later analyzed.

Measurement Items

(1) General Condition Observation: The general condition of the rats was monitored throughout the experiment, including coat quality, mental state, diet, defecation, and joint swelling (swelling = post-modeling diameter – pre-modeling diameter).

(2) Behavioral Assessment: Behavioral indicators, including pain threshold and open field test results, were measured before modeling, on the first day post-modeling, and before tissue collection.

(3) Biochemical Parameters: Blood uric acid levels were measured using an automated biochemical analyzer at baseline, on the first day post-modeling, and before tissue collection. ELISA was used to detect inflammatory cytokine levels, including TNF-α and IL-1β, in the serum.

(4) Immunofluorescence for Kidney Urate Transporter Expression: Immunofluorescence staining was performed on kidney tissues to examine the expression of the urate transporter protein URAT1.

(5) Hematoxylin-Eosin (HE) Staining for Liver and Kidney Histopathology: Liver and kidney tissues were decalcified in EDTA solution until a needle could easily penetrate the tissue. The tissues were then dehydrated, paraffin-embedded, and sectioned into 3 μm slices. After deparaffinization, HE staining was performed, and tissue morphology was examined under 100× and 200× magnification.

(6) Western Blot for Kidney Protein Expression: Kidney tissues were homogenized and lysed at 4°C. After protein separation by electrophoresis and membrane transfer, membranes were blocked at room temperature for 2 hours. Primary antibodies for URAT1 (1:5000) and β-actin (1:5000) were incubated at room temperature for 1 hour and then overnight at 4°C. After washing, secondary antibodies (1:5000) were added for 2 hours at room temperature. Membranes were washed three times, and the protein bands were developed and fixed. Protein expression was quantified using Image J 1.8.0, with β-actin as an internal control.

Statistical Analysis

Statistical analyses and graphical representations were performed using SPSS 23.0 and GraphPad Prism 8.0. Descriptive statistics, including frequency, percentage, mean, and standard deviation, were used for general data. Repeated measures analysis was used for the observation indicators at different time points. For complete data, repeated measures ANOVA was performed, with sphericity tests to assess correlations between repeated measures. If sphericity was violated, the Greenhouse-Geisser correction was applied. If missing data were present, a mixed-effects model was used for analysis. If there was an interaction between group and time effects, multiple *t*-tests were performed at each time point; otherwise, post-hoc comparisons using a stepwise multiple comparison method were applied. For post hoc analysis following significant ANOVA results, Tukey's honestly significant difference (HSD) test was performed to compare pairwise group means.

Results

General Condition of Rats in Each Group

Observations revealed that rats in the control group showed normal weight gain with no other notable changes. In contrast, rats in the model groups exhibited progressively yellowed, dry, and fragile fur, lethargy, increased urination (as evidenced by wet bedding), and sticky or loose stools following model establishment. These symptoms were alleviated to varying degrees in the low-, medium-, and high-dose JBLJQF groups, as well as in the positive drug groups.

Regarding joint swelling, all model groups exhibited significant swelling compared to the control group after modeling. However, after 5 days of treatment, joint swelling in all treatment groups except the benzbromarone group gradually decreased, showing significant differences compared to the model group ($P < 0.05$). See Figure 1.

Histopathological Observations of Kidney, Liver, and Synovial Tissues in Each Group

The pathological states of the kidneys, liver, and synovial tissues in each group were examined. In the control group, the kidney structure was normal, with clear tubule boundaries and tightly arranged renal tubular epithelial cells. The liver tissue exhibited no significant pathological changes, while the synovial cells were orderly arranged, with normal vascular distribution and scattered inflammatory cell infiltration in the surrounding area.

In contrast, the model group showed notable pathological changes compared to the control group. The kidneys exhibited tubular dilation, swelling, degeneration, and necrosis of renal tubular epithelial cells. Liver tissue showed no significant pathological alterations. The synovial tissue revealed extensive inflammatory cell infiltration and synovial tissue hyperplasia.

Compared to the model group, the low-, medium-, and high-dose JBLJQF groups and the benzbromarone group exhibited varying degrees of improvement in the pathological states of the kidneys and synovial tissues. However, in the etoricoxib group, no significant improvements were observed in the pathological states of the kidneys compared to the model group, although this group demonstrated a reduction in inflammatory cell infiltration and synovial tissue hyperplasia, mitigating synovial pathological damage. See Figure 2.

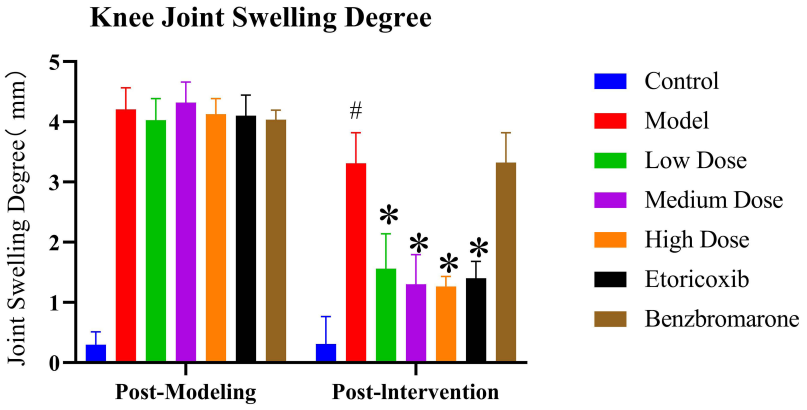

Figure 1 Swelling Degrees of the Knee Joints in Each Group of Rats. #P < 0.05, compared with the control group; *P < 0.05, compared with the model group.

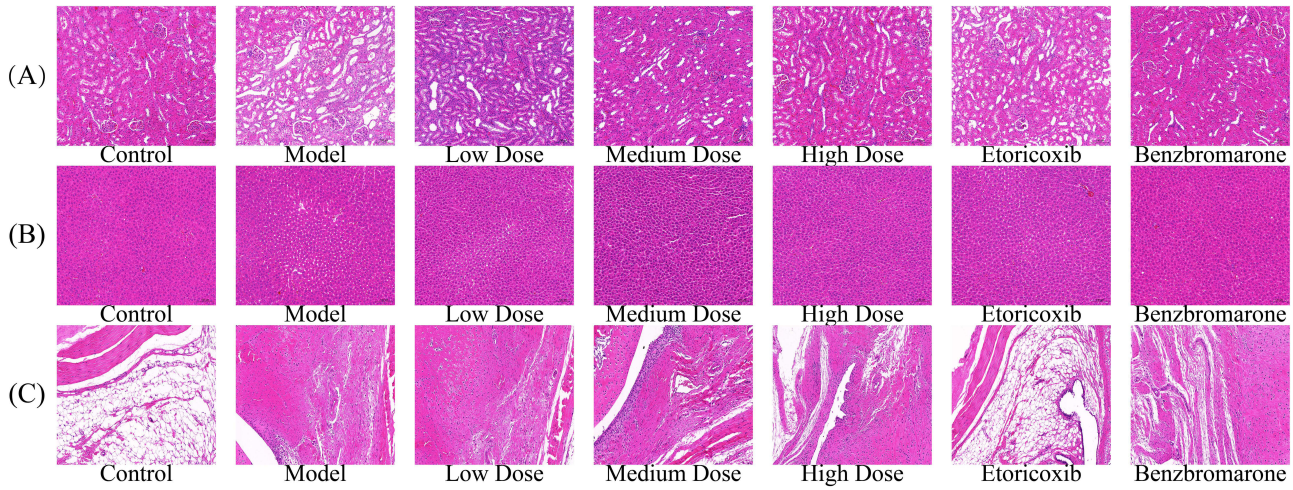

Figure 2 Histopathological Changes in the Kidney, Liver, and Synovial Tissues of Rats in Each Group (×200). (**A**) Kidney, (**B**) Liver, and (**C**) Synovial tissue sections stained with H&E from each group: Control, Model, Low Dose, Medium Dose, High Dose, Etoricoxib, and Benzbromarone.

Behavioral Indicators

Pain Threshold

For the heat pain threshold, a significant decrease was observed in the left hind limb of all model groups compared to the control group after modeling ($P < 0.05$). After 5 days of drug intervention, the heat pain threshold in the left hind limb showed an overall upward trend across all treatment groups. Compared to the model group, the low-, medium-, and high-dose JBLJQF groups and the etoricoxib group exhibited a significant increase in the heat pain threshold ($P < 0.05$). However, in the benzbromarone group, although the heat pain threshold increased after 5 days of intervention, the difference was not statistically significant ($P > 0.05$).

Open Field Test

Total Movement Distance

After modeling, all model groups showed a significant reduction in total movement distance in the open field test compared to the control group ($P < 0.05$). After 5 days of drug intervention, the total movement distance increased in all treatment groups. Compared to the model group, the medium-, and high-dose JBLJQF groups, as well as the etoricoxib group, showed a significant increase in total movement distance ($P < 0.05$), while the low-dose JBLJQF group and the benzbromarone group did not demonstrate a statistically significant difference ($P > 0.05$). See Figure 3.

https://doi.org/10.2147/JPR.S517711

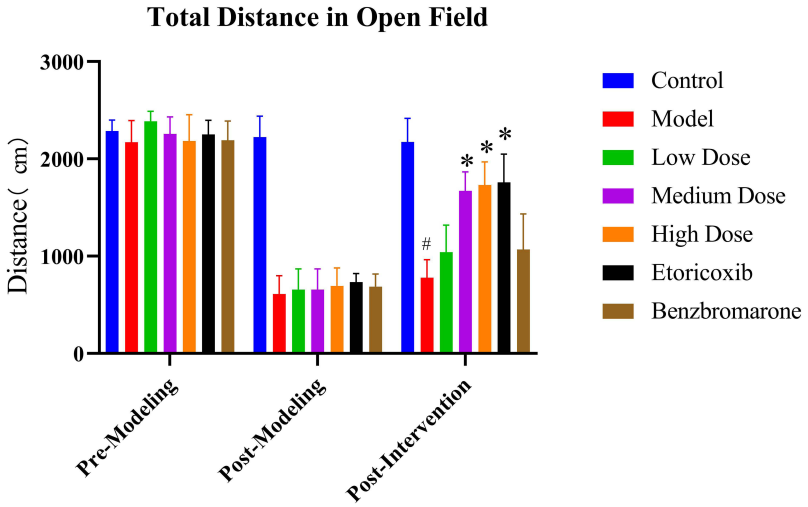

Figure 3 Total Movement Distance. #$P < 0.05$, compared with the control group; *$P < 0.05$, compared with the model group.

Average Speed

After modeling, the average speed in the open field test was significantly reduced in all model groups compared to the control group ($P < 0.05$). After 5 days of drug intervention, the average speed increased across all treatment groups. Compared to the model group, the medium- and high-dose JBLJQF groups and the etoricoxib group exhibited a significant increase in average speed ($P < 0.05$). However, the low-dose JBLJQF group and the benzbromarone group showed no statistically significant differences ($P > 0.05$). See Figure 4.

Immobility Time

After modeling, the immobility time in the open field test significantly increased in all model groups compared to the control group ($P < 0.05$). Following 5 days of drug intervention, the immobility time decreased across all treatment groups. Compared to the model group, the high-dose JBLJQF group and the etoricoxib group showed a significant reduction in immobility time ($P < 0.05$), while the low- and medium-dose JBLJQF groups and the benzbromarone group did not exhibit statistically significant differences ($P > 0.05$). See Figure 5.

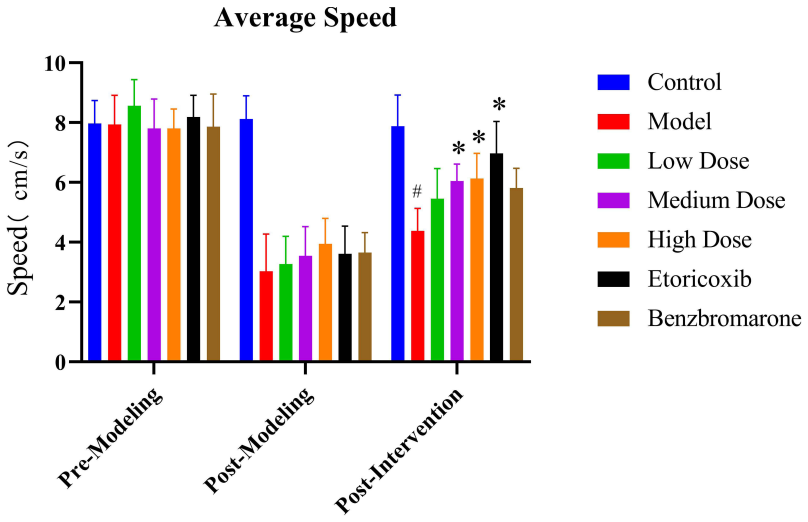

Figure 4 Average Speed. #$P < 0.05$, compared with the control group; *$P < 0.05$, compared with the model group.

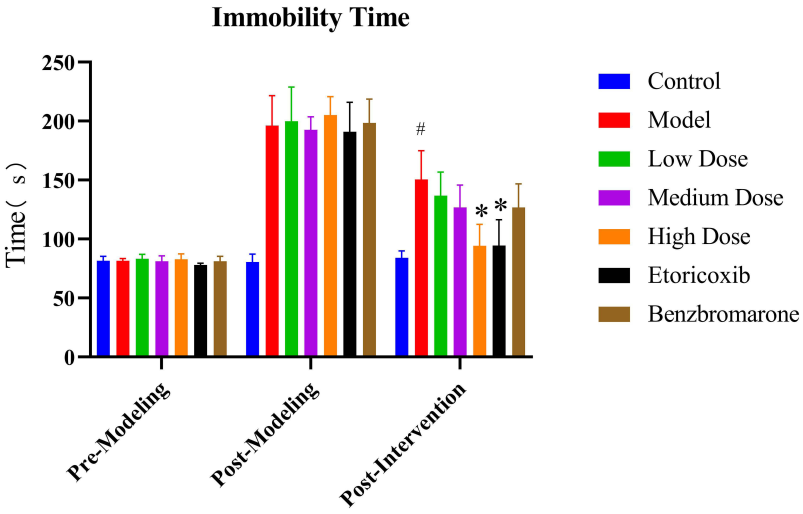

Figure 5 Immobility Time. #*P* < 0.05, compared with the control group; **P* < 0.05, compared with the model group.

Biochemical Indicator Analysis

Serum Uric Acid Levels

See Supplementary Figure 1. After modeling, serum uric acid levels significantly increased in all model groups compared to the control group ($P < 0.05$). Following 5 days of drug intervention, serum uric acid levels decreased in all treatment groups. Compared to the model group, the medium- and high-dose JBLJQF groups, as well as the benzbromarone group, exhibited a significant reduction in serum uric acid levels ($P < 0.05$). However, no statistically significant differences were observed in the low-dose JBLJQF group and the etoricoxib group compared to the model group ($P > 0.05$). Notably, the medium- and high-dose JBLJQF groups and the benzbromarone group showed no significant differences in serum uric acid levels compared to the control group ($P > 0.05$). See Figure 6.

Inflammatory Cytokine Expression

The levels of inflammatory cytokines TNF-α and IL-1β were measured using ELISA. Compared to the control group, all model groups exhibited significantly elevated levels of TNF-α and IL-1β ($P < 0.05$). After 5 days of drug intervention: For TNF-α levels, compared to the model group, the medium- and high-dose JBLJQF groups, as well as the etoricoxib group, showed significant reductions ($P < 0.05$). However, the low-dose JBLJQF group and the benzbromarone group did

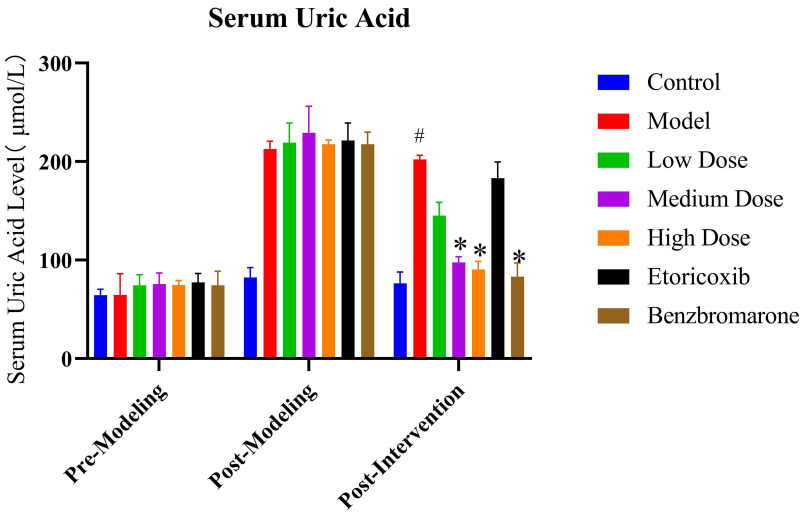

Figure 6 Serum Uric Acid Levels in Each Group of Rats. #*P* < 0.05, compared with the control group; **P* < 0.05, compared with the model group.

https://doi.org/10.2147/JPR.S517711

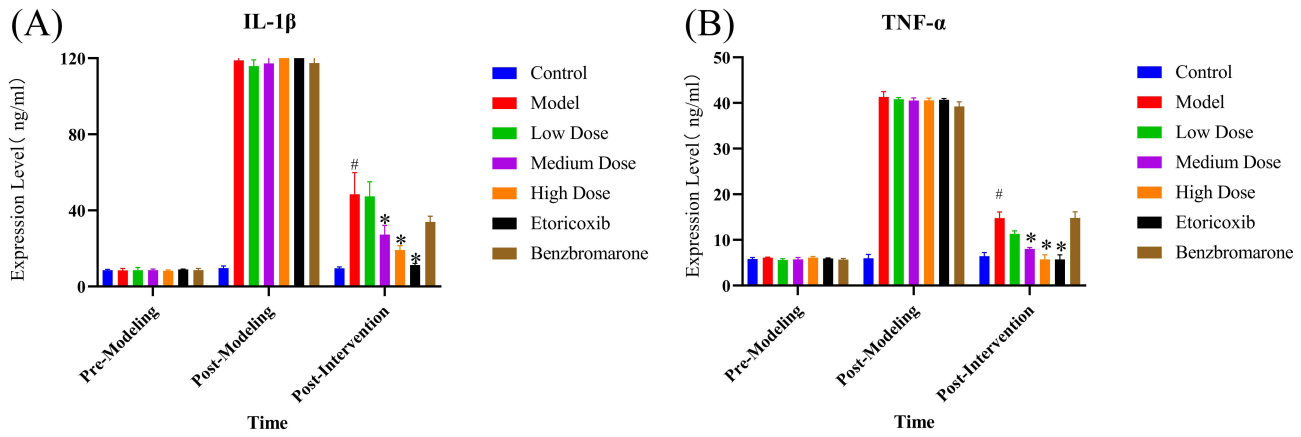

Figure 7 Levels of Inflammatory Cytokines TNF-α and IL-1β in Each Group of Rats. (**A**) Serum IL-1β levels at different time points (pre-modeling, post-modeling, and post-intervention). (**B**) Serum TNF-α levels at different time points (pre-modeling, post-modeling, and post-intervention). #$P < 0.05$, compared with the control group; *$P < 0.05$, compared with the model group.

not exhibit statistically significant differences compared to the model group ($P > 0.05$). Furthermore, the medium- and high-dose JBLJQF groups and the etoricoxib group demonstrated no significant differences compared to the control group after intervention ($P > 0.05$). For IL-1β levels, compared to the model group, the medium- and high-dose JBLJQF groups and the etoricoxib group exhibited significant reductions ($P < 0.05$). In contrast, the low-dose JBLJQF group and the benzbromarone group did not show statistically significant differences compared to the model group ($P > 0.05$). Additionally, the high-dose JBLJQF group and the etoricoxib group showed no significant differences compared to the control group after intervention ($P > 0.05$).See Figure 7.

Immunofluorescence Observation of Renal Urate Transporter Protein Expression

As shown in Figure 8, URAT1 was localized to the basolateral membrane of renal tubular epithelial cells. Compared to the control group, URAT1 protein expression was markedly upregulated in the model group. Treatment with medium and high doses of JBLJQF, as well as benzbromarone, resulted in a progressive reduction in URAT1 expression ($P < 0.05$). However, no statistically significant differences were observed in the low-dose JBLJQF group or the etoricoxib group compared to the model group ($P > 0.05$).

URAT1 Protein Expression Levels

Compared to the control group, URAT1 expression was significantly upregulated in the model group ($P < 0.01$). In comparison to the model group, URAT1 expression was significantly downregulated in the medium- and high-dose JBLJQF groups and the benzbromarone group ($P < 0.01$). The low-dose JBLJQF group showed a slight reduction in URAT1 expression, but the difference was not statistically significant. See Figure 9.

Discussion

Hyperuricemia plays a central role in the pathogenesis of gouty arthritis (GA), primarily inducing acute inflammatory responses within joints through the deposition of monosodium urate crystals. The prevalence of GA ranges from <1% to 6.8%, with an incidence rate of 0.58–2.89 per 1000 person-years.[15,16] Clinically, mainstream treatments for GA with hyperuricemia typically include nonsteroidal anti-inflammatory drugs (NSAIDs), colchicine, and uric acid-lowering agents such as benzbromarone.[17] These drugs have demonstrated significant efficacy in alleviating acute gout flares and reducing serum uric acid levels. However, NSAIDs and colchicine are primarily used to manage acute symptoms, and their long-term use may lead to gastrointestinal discomfort, hepatic and renal damage, and other side effects.[18] Although uric acid-lowering agents can effectively reduce serum uric acid, their safety risks remain a concern.[19] Therefore, it is clinically important to explore therapies that balance anti-inflammatory effects, uric acid reduction, and organ protection.

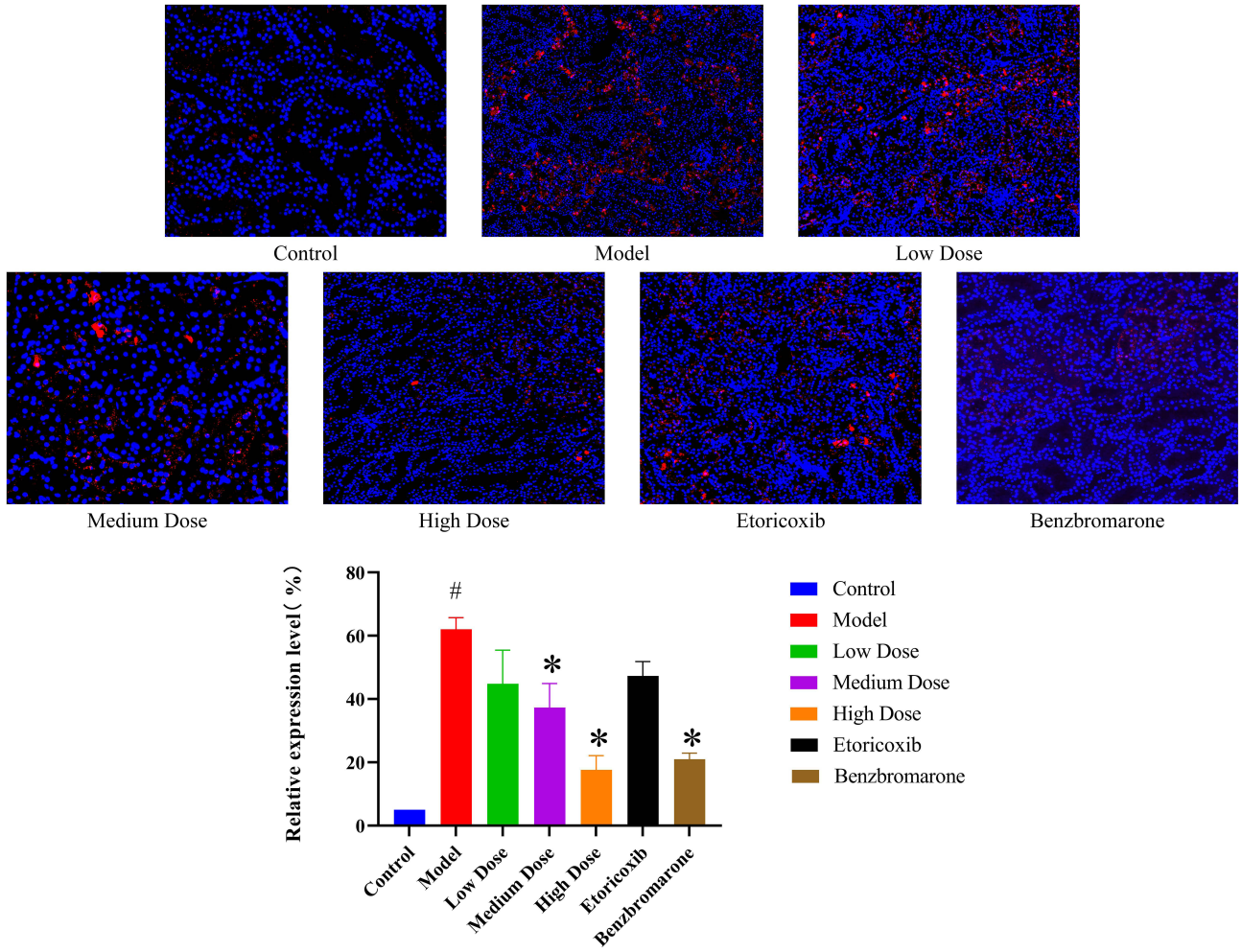

Figure 8 URAT1 Expression in Each Group of Rats. Blue fluorescence (DAPI staining) indicates cell nuclei, while red fluorescence represents URAT1 expression. #$P < 0.05$, compared with the control group; *$P < 0.05$, compared with the model group.

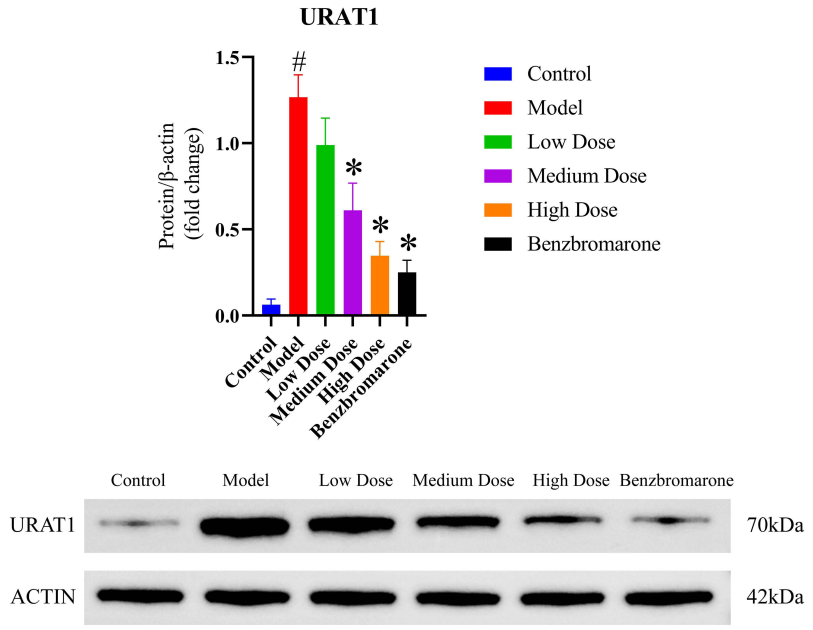

Figure 9 URAT1 Protein Expression Levels in Each Group of Rats. #$P < 0.05$, compared with the control group; *$P < 0.05$, compared with the model group.

https://doi.org/10.2147/JPR.S517711

Traditional Chinese medicine (TCM) offers unique advantages, including multi-target effects and low toxicity, making it a promising candidate for achieving anti-inflammatory, uric acid-lowering, and organ-protective effects. Previous studies have shown that JBLJQF may alleviate acute gouty arthritis (AGA) by inhibiting the NLRP3 inflammasome signaling pathway, thereby reducing the expression of NLRP3, ASC, and Caspase-1, suppressing the maturation of IL-1β, and mitigating local inflammation.[20] Additionally, JBLJQF has been shown to inhibit the expression of TLR4 mRNA, MyD88, and IKK-β proteins while upregulating IκB-α protein, suggesting that its anti-inflammatory effects may be mediated through the MyD88-dependent pathway.[21] Furthermore, JBLJQF may exert anti-inflammatory effects by upregulating PPARγ, which inhibits the expression of TLR4 and NF-κB, thereby further reducing local inflammation in AGA.[22,23]

In this study, four major findings were identified. First, JBLJQF significantly improved the general condition of GA rats with hyperuricemia, including coat quality, mental state, and bowel and urinary functions. Compared to the model group, all JBLJQF dose groups reduced joint swelling to varying degrees and alleviated pathological damage to the kidneys and synovial tissues. Second, in terms of behavioral indicators, the medium- and high-dose JBLJQF groups significantly increased the heat pain threshold and improved motor abilities in the model rats, including increased total movement distance and average speed and reduced immobility time (high-dose group). These results indicate that JBLJQF has a positive effect on relieving pain and improving mobility in GA. Third, biochemical analysis showed that the medium- and high-dose JBLJQF groups significantly reduced serum uric acid levels, with no significant difference compared to the control group. Additionally, JBLJQF significantly inhibited the expression of inflammatory cytokines TNF-α and IL-1β, demonstrating robust anti-inflammatory effects. Finally, immunofluorescence and Western blot results showed that JBLJQF reduced URAT1 expression in the kidneys in a dose-dependent manner, suggesting that the formula may achieve uric acid-lowering effects by regulating uric acid metabolism pathways.

Numerous studies have demonstrated that TNF-α and IL-1β play critical roles in promoting inflammation during gout flares, particularly when monosodium urate crystals are deposited in joints, triggering acute inflammatory responses.[24,25] The significant reduction in these inflammatory cytokines by JBLJQF suggests that the formula may protect joint tissues by inhibiting the inflammatory cascade. Improvements in behavioral indicators are likely associated with reduced inflammation and alleviated joint swelling.[26,27] Further research into the molecular mechanisms underlying the effects of JBLJQF on function and pain threshold may enhance our understanding of its therapeutic potential.

URAT1 is a key transporter in renal uric acid reabsorption.[28,29] Located on the apical membrane of renal proximal tubular epithelial cells, URAT1 facilitates the reabsorption of uric acid. Hyperuricemia is primarily caused by increased uric acid reabsorption mediated by URAT1, which promotes uric acid crystal deposition and leads to GA.[30] In this study, JBLJQF was found to downregulate URAT1 expression in the kidneys, suggesting that its regulation of URAT1 may facilitate uric acid excretion and help maintain normal uric acid levels.

In recent years, increasing attention has been directed toward the role of energy metabolism-related pathways in the regulation of uric acid homeostasis. It has been demonstrated that activation of AMP-activated protein kinase (AMPK) upregulates nuclear factor erythroid 2–related factor 2 (Nrf2), which subsequently enhances the expression of the urate efflux transporter ABCG2 in renal and intestinal tissues, thereby promoting uric acid excretion.[31] In addition to the AMPK/Nrf2 axis, the metabolic sensor Silent Information Regulator 1 (SIRT1) has also been identified as a key protective factor in hyperuricemia. Activation of SIRT1 improves mitochondrial function and attenuates oxidative stress and inflammatory responses, contributing to the modulation of urate metabolism.[32] Furthermore, sodium-glucose cotransporter 2 (SGLT2) inhibitors, a class of antidiabetic agents that modulate glucose metabolism, have been shown to reduce the flux through the pentose phosphate pathway, thereby limiting purine and uric acid synthesis while simultaneously promoting renal urate excretion.[33,34] However, whether JBLJQF modulates urate excretion through similar energy metabolism–related pathways remains unclear, and warrants further investigation.

In addition to URAT1, other transporters such as GLUT9, OAT1, OAT3, and ABCG2 also play crucial roles in the reabsorption and excretion of uric acid.[35,36] Although the present study primarily focuses on the expression changes of URAT1, it is plausible that JBLJQF may exert its urate-lowering effect through the modulation of multiple uric acid transporters. This hypothesis warrants further investigation to comprehensively elucidate its multi-target regulatory mechanisms in uric acid metabolism. Notably, inflammation not only contributes to local joint damage but may also

influence the expression levels of renal urate transporters through cytokine-mediated pathways. Ying Yang et al reported that Wuling San may ameliorate fructose-induced hyperuricemic nephropathy by suppressing the TLR4/MyD88/NLRP3 signaling pathway and regulating renal urate transporters.[37] Similarly, Ming-Xing Wang et al found that nuciferine alleviates renal inflammation in hyperuricemic mice by inhibiting the TLR4/MyD88/NF-κB and NLRP3 pathways, thereby reducing IL-1β expression and modulating urate transporter activity.[38] These findings suggest that JBLJQF may enhance uric acid excretion and regulate serum uric acid levels by modulating the expression of urate transporters such as URAT1 through alleviation of the inflammatory microenvironment. This implies a potential functional interplay between anti-inflammatory effects and uric acid regulation, providing a theoretical basis for the multifaceted mechanisms of JBLJQF.

The strength of this study lies in its mechanistic exploration of JBLJQF in the treatment of GA complicated with hyperuricemia, based on previously validated clinical efficacy. To our knowledge, this is the first study to systematically integrate behavioral assessments, biochemical indices, histopathological evaluation, and molecular analyses in an animal model, thereby comprehensively demonstrating the multifaceted pharmacological effects of JBLJQF in anti-inflammation, uric acid reduction, and multi-organ protection. The results showed that JBLJQF significantly improved the general condition and joint symptoms in model rats, enhanced their locomotor function, suppressed inflammatory cytokine expression, and reduced renal URAT1 expression. These findings suggest that JBLJQF may exert its therapeutic effects through a multi-target synergistic mechanism. In addition, the use of a dose-gradient design confirmed the dose-dependent efficacy of JBLJQF, providing important preclinical evidence for future dose optimization and clinical application. Although this study has clarified several important mechanisms of action, there is still room for further investigation. First, whether JBLJQF regulates uric acid metabolism through energy metabolism related pathways such as AMPK/Nrf2, SIRT1, or SGLT2 was not explored in the present study. These pathways have recently attracted increasing attention in the regulation of hyperuricemia and should be investigated further using metabolomics and molecular biology techniques. Second, as a traditional Chinese medicine compound, the therapeutic effects of JBLJQF may result from synergistic actions of multiple components. Future studies are encouraged to isolate and identify key active monomeric constituents, which would help improve its quality control and advance mechanistic research in a more precise and modern framework.

In conclusion, JBLJQF demonstrates multi-target effects, including anti-inflammatory, uric acid-lowering, and organ-protective properties, highlighting its potential as a therapeutic agent for GA with hyperuricemia. Further studies to isolate the active components of JBLJQF and investigate their precise cellular and molecular mechanisms will provide deeper insights into its multi-target effects.

Conclusion

This study demonstrated that JBLJQF exhibits significant anti-inflammatory, uric acid-lowering, and multi-organ protective effects in a rat model of gouty arthritis with hyperuricemia. By regulating URAT1 expression and inhibiting inflammatory cytokines, JBLJQF offers a potential low-toxicity, multi-target therapeutic approach for this condition. Although this study has systematically elucidated the major mechanisms of action, it has not yet addressed whether JBLJQF regulates uric acid metabolism through energy metabolism–related pathways. In addition, its specific active constituents remain to be isolated and identified. Future studies should further investigate these mechanisms and validate the efficacy and safety of JBLJQF through clinical trials, thereby supporting its standardized application in clinical practice.

Data Sharing Statement

No data was used for the research described in the article.

Ethics Approval and Consent to Participate

This animal study was approved by the Animal Ethics Committee of Hunan University of Chinese Medicine (HNUCM21-2404-202).

Acknowledgment

The authors declare financial support was received for the research, authorship, and/or publication of this article. This work was supported by Natural Science Foundation of China (NSFC) (81574005) and Project of the Education Department of Hunan Province of China (23B0343, 23C0179) and Key R&D Projects in Hunan Province in 2023 Scientific Research of China (2023SK2047) and Changsha City Science and Technology Program Project of China (kh2201056) and Hunan Provincial Chinese Medicine Research Plan Project (C2023031, D2022033) and Hunan University of Chinese Medicine School-level Research Project (2022XJZK003) and Graduate Student Innovation Project of Hunan University of Chinese Medicine of China (2023CX23) and Hunan Provincial Natural Science Foundation (2024JJ6342).

Author Contributions

All authors made a significant contribution to the work reported, whether that is in the conception, study design, execution, acquisition of data, analysis and interpretation, or in all these areas; took part in drafting, revising or critically reviewing the article; gave final approval of the version to be published; have agreed on the journal to which the article has been submitted; and agree to be accountable for all aspects of the work.

Disclosure

The authors report no conflicts of interest in this work.

References

1. Dalbeth N, Gosling AL, Gaffo A, Abhishek A. Gout. *Lancet*. 2021;397(10287):1843–1855. doi:10.1016/S0140-6736(21)00569-9
2. Sellin L, Kielstein JT, de Groot K. Hyperuricemia - more than gout: impact on cardiovascular risk and renal insufficiency. *Z Rheumatol*. 2015;74(4):322–328. doi:10.1007/s00393-014-1481-1
3. Jaruvongvanich V, Ahuja W, Wirunsawanya K, Wijarnpreecha K, Ungprasert P. Hyperuricemia is associated with nonalcoholic fatty liver disease activity score in patients with nonalcoholic fatty liver disease: a systematic review and meta-analysis. *Eur J Gastroenterol Hepatol*. 2017;29(9):1031–1035. doi:10.1097/MEG.0000000000000931
4. Roddy E, Bajpai R, Forrester H, et al. Safety of colchicine and NSAID prophylaxis when initiating urate-lowering therapy for gout: propensity score-matched cohort studies in the UK Clinical Practice Research Datalink. *Ann Rheum Dis*. 2023;82(12):1618–1625. doi:10.1136/ard-2023-224154
5. Lin TM, Chi JE, Chang CC, Kang YN. Do etoricoxib and indometacin have similar effects and safety for gouty arthritis? A meta-analysis of randomized controlled trials. *J Pain Res*. 2019;12:83–91. doi:10.2147/JPR.S186004
6. Lin N, Dai Q, Zhang Y, Xu L. Chinese classical decoction Wuwei Xiaodu Drink alleviates gout arthritis by suppressing NLRP3-Mediated inflammation. *Front Pharmacol*. 2024;15:1388753. doi:10.3389/fphar.2024.1388753
7. Bian M, Zhu C, Nie A, Zhou Z. Guizhi Shaoyao Zhimu Decoction ameliorates gouty arthritis in rats via altering gut microbiota and improving metabolic profile. *Phytomedicine*. 2024;131:155800. doi:10.1016/j.phymed.2024.155800
8. Peng S, Tian J, Jin L, et al. Efficacy and safety of Danggui Niantong Decoction in patients with gout: a systematic review and meta-analysis. *Front Pharmacol*. 2023;14:1168863. doi:10.3389/fphar.2023.1168863
9. Lin X, Wang M, He Z, Hao G. Gut microbiota mediated the therapeutic efficiency of Simiao decoction in the treatment of gout arthritis mice. *BMC Complement Med Ther*. 2023;23(1):206. doi:10.1186/s12906-023-04042-4
10. Fan QQ, Zhai BT, Zhang D, et al. Study on the Underlying Mechanism of Yinhua Gout Granules in the Treatment of Gouty Arthritis by Integrating Transcriptomics and Network Pharmacology. *Drug Des Devel Ther*. 2024;18:3089–3112. doi:10.2147/DDDT.S475442
11. Hao W, Hui X, Qing F, et al. Clinical effect of Juanbi Lijieqing prescription in treatment of gouty arthritis with heat stasis syndrome: an analysis of 31 cases. *Hunan J Tradit Chin Med*. 2018;34(06):12–15. doi:10.16808/j.cnki.issn1003-7705.2018.06.005
12. Nan S, Wei L, Hui X, et al. Efficacy observation of Juanbi Lijieqing formula and Xiaoyan powder on acute gouty arthritis with syndrome of accumulated damp-heat. *Shanxi J Tradit Chin Med*. 2023;39(05):22–24. doi:10.20002/j.issn.1000-7156.2023.05.009
13. Zhi T, Hui X, Xiaolong L, et al. Combination of Juanbi Lijieqing formula and ozone therapy for gouty knee arthritis. *Lishizhen Med Mater Med Res*. 2019;30(12):2865–2867.
14. Zhennan Q, Hui X, Xiaolong L, et al. Clinical effect of Juanbi Lijieqing prescription combined with acupuncture in treatment of acute gouty arthritis with damp-heat accumulation: an analysis of 31 cases. *Hunan J Tradit Chin Med*. 2019;35(11):10–12. doi:10.16808/j.cnki.issn1003-7705.2019.11.004
15. Dehlin M, Jacobsson L, Roddy E. Global epidemiology of gout: prevalence, incidence, treatment patterns and risk factors. *Nat Rev Rheumatol*. 2020;16(7):380–390. doi:10.1038/s41584-020-0441-1
16. Zhou X, Liu K, Shi C, et al. Estimation of the spatial pattern of gout prevalence across China by wastewater-based epidemiology. *Sci Total Environ*. 2024;924:171565. doi:10.1016/j.scitotenv.2024.171565
17. Peng X, Li X, Xie B, et al. Gout therapeutics and drug delivery. *J Control Release*. 2023;362:728–754. doi:10.1016/j.jconrel.2023.09.011
18. Grahame R. Is there still a place for colchicine in the treatment of acute gout. *Int J Clin Pract*. 2007;61(12):1966–1967. doi:10.1111/j.1742-1241.2007.01556.x
19. Stamp LK. Safety profile of anti-gout agents: an update. *Curr Opin Rheumatol*. 2014;26(2):162–168. doi:10.1097/BOR.0000000000000031

20. Yuanhang Z, Xiaoyu Y, Peng G, et al. Study of Juanbi Lijieqing Decoction on NLRP3 inflammatory body inhibition in rats with acute gouty arthritis. *J Emerg Tradit Chin Med*. 2022;31(01):76–79+90. doi:10.3969/j.issn.1004-745X.2022.01.018
21. Yuxing G, Biao Z, Hui X, et al. The effect of Juanbi Lijieqing formula on key components of the TLR4/NF-κB signaling pathway in a gout cell model. *Chin J Pharmacol Clin Ther Tradit Chin Med*. 2019;35(01):155–160. doi:10.13412/j.cnki.zyyl.2019.01.034
22. Yuxing G, Hui X, Fayin Y, et al. The effects of Juanbi Lijieqing formula on PPARγ, TLR4, and NF-κB in a gout cell model. *Chin J Exp Tradit Med Formulae*. 2018;24(23):126–133. doi:10.13422/j.cnki.syfjx.20182332
23. Qin Y, Zhou Y, Xiong J, et al. Limosilactobacillus reuteri RE225 alleviates gout by modulating the TLR4/MyD88/NF-κB inflammatory pathway and the Nrf2/HO-1 oxidative stress pathway, and by regulating gut microbiota. *J Sci Food Agric*. 2025;105(2):1185–1193. doi:10.1002/jsfa.13908
24. Chen CJ, Shi Y, Hearn A, et al. MyD88-dependent IL-1 receptor signaling is essential for gouty inflammation stimulated by monosodium urate crystals. *J Clin Invest*. 2006;116(8):2262–2271. doi:10.1172/JCI28075
25. Liao XZ, Xie RX, Zheng SY, et al. Bioinformatics and molecular docking reveal Cryptotanshinone as the active anti-inflammation component of Qu-Shi-Xie-Zhuo decoction by inhibiting S100A8/A9-NLRP3-IL-1β signaling. *Phytomedicine*. 2024;136:156257. doi:10.1016/j.phymed.2024.156257
26. Selvadurai D, Coleshill MJ, Day RO, et al. Patient factors and health outcomes associated with illness perceptions in people with gout. *Rheumatology*. 2024;63(7):1927–1937. doi:10.1093/rheumatology/kead501
27. Dalbeth N, Petrie KJ, House M, et al. Illness perceptions in patients with gout and the relationship with progression of musculoskeletal disability. *Arthritis Care Res*. 2011;63(11):1605–1612. doi:10.1002/acr.20570
28. Nakanishi T, Ohya K, Shimada S, Anzai N, Tamai I. Functional cooperation of URAT1 (SLC22A12) and URATv1 (SLC2A9) in renal reabsorption of urate. *Nephrol Dial Transplant*. 2013;28(3):603–611. doi:10.1093/ndt/gfs574
29. Kaufmann D, Chaiyakunapruk N, Schlesinger N. Optimizing Gout Treatment: a Comprehensive Review of Current and Emerging Uricosurics. *Joint Bone Spine*. 2024;105826. doi:10.1016/j.jbspin.2024.105826
30. Hou Z, Ma A, Mao J, Song D, Zhao X. Overview of the pharmacokinetics and pharmacodynamics of URAT1 inhibitors for the treatment of hyperuricemia and gout. *Expert Opin Drug Metab Toxicol*. 2023;19(12):895–909. doi:10.1080/17425255.2023.2287477
31. Song K, Kong X, Zhang Z, et al. Sleeve gastrectomy ameliorates renal injury in obesity-combined hyperuricemic nephropathy mice by modulating the AMPK/Nrf2/ABCG2 pathway. *Sci Rep*. 2024;14(1):22834. doi:10.1038/s41598-024-73807-9
32. Lu C, Zhao H, Liu Y, et al. Novel Role of the SIRT1 in Endocrine and Metabolic Diseases. *Int J Biol Sci*. 2023;19(2):484–501. doi:10.7150/ijbs.78654
33. Lopaschuk GD, Verma S. Mechanisms of Cardiovascular Benefits of Sodium Glucose Co-Transporter 2 (SGLT2) Inhibitors: a State-of-the-Art Review. *JACC Basic Transl Sci*. 2020;5(6):632–644. doi:10.1016/j.jacbts.2020.02.004
34. Packer M. Hyperuricemia and Gout Reduction by SGLT2 Inhibitors in Diabetes and Heart Failure: JACC Review Topic of the Week. *J Am Coll Cardiol*. 2024;83(2):371–381. doi:10.1016/j.jacc.2023.10.030
35. Matsushita D, Toyoda Y, Lee Y, et al. Structural basis of urate transport by glucose transporter 9. *Cell Rep*. 2025;44(4):115514. doi:10.1016/j.celrep.2025.115514
36. Guo W, Wei M, Li Y, et al. Mechanisms of urate transport and uricosuric drugs inhibition in human URAT1. *Nat Commun*. 2025;16(1):1512. doi:10.1038/s41467-025-56843-5
37. Yang Y, Zhang DM, Liu JH, et al. Wuling San protects kidney dysfunction by inhibiting renal TLR4/MyD88 signaling and NLRP3 inflammasome activation in high fructose-induced hyperuricemic mice. *J Ethnopharmacol*. 2015;169:49–59. doi:10.1016/j.jep.2015.04.011
38. Wang MX, Liu YL, Yang Y, Zhang DM, Kong LD. Nuciferine restores potassium oxonate-induced hyperuricemia and kidney inflammation in mice. *Eur J Pharmacol*. 2015;747:59–70. doi:10.1016/j.ejphar.2014.11.035